Enhancing OFDM with index modulation using heuristic geometric constellation shaping and generalized interleaving for underwater VLC

YINAN ZHAO, 1 CHEN CHEN, 1,4 D XIN ZHONG, 1 HAILIN CAO, 1 MIN LIU, 1 BANGJIANG LIN, 2,5 D AND SVETISLAV SAVOVIĆ 3 D

Abstract: In this paper, we propose and demonstrate enhanced orthogonal frequency division multiplexing with index modulation (OFDM-IM) schemes for bandlimited underwater visible light communication (UVLC) systems via geometric constellation shaping (GCS) and subblock interleaving. Specifically, two heuristic GCS approaches based on particle swarm optimization (PSO) and hybrid genetic algorithm-PSO (GA-PSO) algorithms are proposed to generate IMpreferable constellations. Moreover, a generalized interleaving technique is further proposed to overcome the low-pass effect of bandlimited UVLC systems, where an optimal step size can be obtained to perform subblock interleaving. Simulation and experiments are conducted to evaluate the performance of the proposed enhanced OFDM-IM schemes in bandlimited UVLC systems, where both OFDM with single-mode index modulation (OFDM-SM) and OFDM with dual-mode index modulation (OFDM-DM) schemes are considered. The experimental results demonstrate remarkable signal-to-noise ratio (SNR) gains of 1.3 and 1.9 dB for OFDM-SM and OFDM-DM in comparison to the benchmark schemes, respectively.

© 2024 Optica Publishing Group under the terms of the Optica Open Access Publishing Agreement

Introduction

As a promising communication technology for practical underwater environments, underwater visible light communication (UVLC) has attracted significant attention in recent years [1,2]. Compared with traditional underwater acoustic and radio frequency communications, UVLC enjoys many unique advantages such as large bandwidth, high data rate, low propagation latency, high security, small size, and low power consumption [3,4]. Nevertheless, commercial off-theshelf light sources such as light-emitting diodes (LEDs) and laser diodes (LDs) usually have a limited bandwidth which exhibit a typical low-pass frequency response, especially for illumination LEDs [5]. Therefore, it is of practical significance to boost the capacity of bandlimited low-pass UVLC systems for a given modulation bandwidth.

Owing to its high spectral efficiency, simple single-tap equalization and flexibility to enable multi-user access, orthogonal frequency division multiplexing (OFDM) has been widely introduced to improve the performance of UVLC systems [6,7]. Lately, OFDM with index modulation (OFDM-IM) has been proposed to enhance the performance of classical OFDM by performing index modulation among a group of subcarriers [8]. Particularly, OFDM with single-mode index modulation (OFDM-SM) can obtain better bit error rate (BER) performance than classical OFDM [9], while OFDM with dual-mode index modulation (OFDM-DM) can achieve higher spectral efficiency than classical OFDM [10]. Due to the superior performance of OFDM-SM

¹School of Microelectronics and Communication Engineering, Chongqing University, Chongqing 400044, China

 $^{^2}$ Quanzhou Institute of Equipment Manufacturing, Haixi Institutes, Chinese Academy of Sciences, Quanzhou, Fujian, China

³University of Kragujevac, Faculty of Science, R. Domanovića 12, Kragujevac, Serbia

⁴c.chen@cqu.edu.cn

⁵linbangjiang@fjirsm.ac.cn

and OFDM-DM, they have also been considered in various VLC systems [11–14]. Moreover, considering the complex and dynamic underwater environments, OFDM-IM techniques have also been applied for performance improvement of UVLC systems [15]. Specifically, a unipolar X-transform based OFDM-SM has been proposed in [16], which can reduce the peak-to-average power ratio (PAPR) of the signal and improve the BER performance. In [17], dual-frame OFDM-DM has been designed to realize 0.5-bit/s/Hz fine-grained adaptive OFDM modulation so as to enhance the bandwidth utilization and hence improve the capacity of bandlimited low-pass UVLC systems.

For both OFDM-SM and OFDM-DM, the constellation design plays a vital role to yield satisfactory BER performance. So far, very little work has been done regarding the constellation design for OFDM-SM and OFDM-DM in VLC or UVLC systems. In [18], a partitioning-based constellation design approach has been proposed for OFDM-DM in VLC systems, which has been shown to outperform the block-based constellation design approach due to the enlarged minimum Euclidean distance. Nevertheless, the partitioning-based constellation design is still based on the conventional rectangular quadrature amplitude modulation (QAM) constellations, and the resultant constellation design might not be able to achieve the optimal performance. As a promising technique to shape the constellations, geometric constellation shaping (GCS) has been widely applied in optical fiber communication systems [19,20] and VLC/UVLC systems [21,22]. Moreover, multi-dimensional GCS has been further proposed to harvest more shaping gains [23–25]. However, these reported GCS techniques are mostly used to shape the standard QAM constellations, which are not directly applicable for OFDM-IM since the constellation design in OFDM-IM needs to be conducted with respect to each subblock consisting of multiple subcarriers. Apart from constellation design, the performance of both OFDM-SM and OFDM-DM is also significantly affected by the low-pass frequency response of bandlimited UVLC systems. To overcome the adverse low-pass effect, discrete Fourier transform (DFT) spreading has been applied to OFDM-SM and OFDM-DM in VLC systems [14,18]. However, the use of DFT spreading transforms the multi-carrier OFDM signal to a quasi-single-carrier signal, which cannot flexibly enable multi-user access. Besides, subblock interleaving has also been considered to mitigate the low-pass effect for OFDM-SM and OFDM-DM in VLC systems [26,27]. Compared with DFT spreading, subblock interleaving can not only realize low-pass effect mitigation but also enable flexible multi-user access [26]. However, traditional interleaving cannot adapt to the distinctive low-pass profile of the system, which might limit the achievable performance gain of subblock interleaving.

To address both the constellation design and low-pass mitigation issues for OFDM-IM, in this paper, we for the first time propose enhanced OFDM-IM schemes for bandlimited UVLC systems, where both OFDM-SM and OFDM-DM are taken into consideration. For the constellation design issue, two heuristic GCS approaches are proposed to optimize the constellations for both OFDM-SM and OFDM-DM. For the low-pass mitigation issue, a generalized interleaving technique is further proposed to achieve improved performance than traditional interleaving. Both simulations and experiments are conducted to verify the feasibility and superiority of the proposed enhanced OFDM-IM schemes in bandlimited UVLC systems.

2. Principle

2.1. Enhanced OFDM-IM

Figure 1 depicts the block diagram of the proposed enhanced OFDM-IM scheme for bandlimited UVLC systems. At the transmitter side, m input bits are partitioned into G groups via a bit splitter, and each group has b bits (b = m/G), which are sent into a subblock. Within each subblock, b bits are further split into two parts, b_i and b_c , fed into an index selector and an SM/DM constellation mapper, respectively. The length of each subblock is N, where $N = N_{\rm data}/G$ and $N_{\rm data}$ represents the number of data subcarriers.

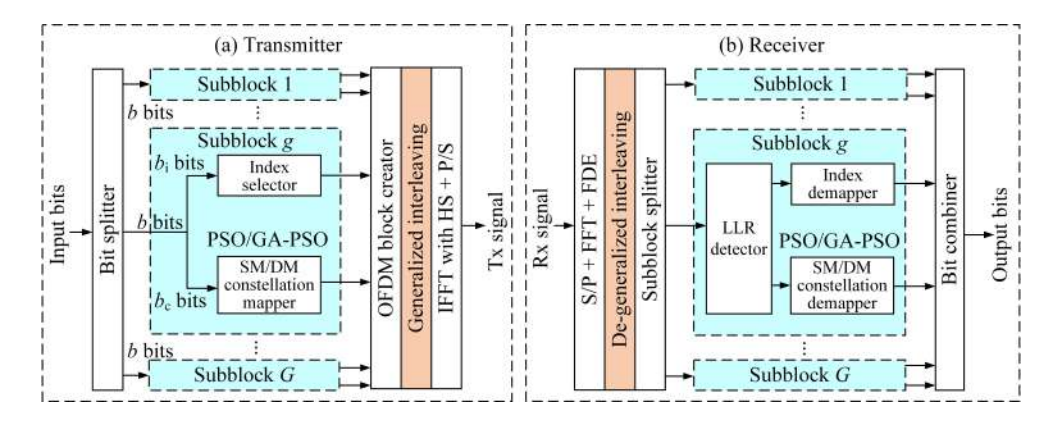


Fig. 1. Block diagram of enhanced OFDM-IM: (a) transmitter and (b) receiver.

For OFDM-SM, the constellation set $\mathcal{M} = [S_1, S_2, \dots, S_M]$ with size M is transmitted by the selected k subcarriers, while no data is transmitted by the non-selected N-k subcarriers within each subblock. The mapping table of OFDM-SM for N=4 and k=2 is given in Table 1. For OFDM-DM, the constellation sets $\mathcal{M}_A = \left[S_1^A, S_2^A, \dots, S_{M_A}^A\right]$ and $\mathcal{M}_B = \left[S_1^B, S_2^B, \dots, S_{M_B}^B\right]$ are transmitted by the selected k subcarriers and the non-selected N-k subcarriers within each subblock, respectively. The sizes of \mathcal{M}_A and \mathcal{M}_B are respectively denoted by M_A and M_B , and we have $\mathcal{M}_A \cap \mathcal{M}_B = \varnothing$. The design of two distinguishable constellation sets \mathcal{M}_A and \mathcal{M}_B plays a vital role in OFDM-DM, which will be discussed in detail in Section 2.2. The mapping table of OFDM-DM for N=4 and k=2 is given in Table 2. After index selection and SM/DM constellation mapping, a total of G subblocks are generated which are further concatenated by a subblock combiner to create a complete OFDM block. Subsequently, generalized interleaving is conducted to mitigate the adverse low-pass effect of the overall system. Finally, the transmitted signal is generated after performing inverse fast Fourier transform (IFFT) with Hermitian symmetry (HS) and parallel-to-serial (P/S) conversion.

Table 1. Mapping table of OFDM-SM for N=4 and k=2

Index bits	Index set for \mathcal{M}	Subblocks	
00	[1,2]	$[S_i, S_j, 0, 0]$	
01	[2, 3]	$[0, S_i, S_j, 0]$	
11	[3,4]	$[0,0,S_i,S_j]$	
10	[1,4]	$[S_i, 0, 0, S_j]$	

Table 2. Mapping table of OFDM-DM for N=4 and k=2

Index bits	Index set for \mathcal{M}_A	Index set for \mathcal{M}_B	Subblocks
00	[1, 2]	[3,4]	$\left[S_i^{\mathrm{A}}, S_j^{\mathrm{A}}, S_i^{\mathrm{B}}, S_j^{\mathrm{B}}\right]$
01	[2, 3]	[1,4]	$\left[S_i^{\mathrm{B}}, S_i^{\mathrm{A}}, S_j^{\mathrm{A}}, S_j^{\mathrm{B}}\right]$
11	[3,4]	[1, 2]	$S_i^{\mathrm{B}}, S_j^{\mathrm{B}}, S_i^{\mathrm{A}}, S_j^{\mathrm{A}}$
10	[1,4]	[2, 3]	$\begin{bmatrix} S_{i}^{A}, S_{j}^{A}, S_{i}^{B}, S_{j}^{B} \\ S_{i}^{B}, S_{i}^{A}, S_{j}^{A}, S_{j}^{B} \\ S_{i}^{B}, S_{j}^{B}, S_{i}^{A}, S_{j}^{A} \end{bmatrix}$ $\begin{bmatrix} S_{i}^{B}, S_{j}^{B}, S_{j}^{A}, S_{j}^{A} \\ S_{i}^{A}, S_{i}^{B}, S_{j}^{B}, S_{j}^{A} \end{bmatrix}$

At the receiver side, the received signal undergoes serial-to-parallel (S/P) conversion, fast Fourier transform (FFT), frequency-domain equalization (FDE), and de-generalized interleaving. The OFDM block is then divided into G subblocks using a subblock splitter. Within each

subblock, a low-complexity log-likelihood ratio (LLR) detector is adopted for signal detection [14,18]. After index demapping and SM/DM constellation demapping, the transmitted bits of each subblock can be recovered. Finally, the output bits are obtained by combining the recovered bits of all the *G* subblocks via a bit combiner.

2.2. Heuristic geometric constellation shaping (GCS)

The performance of OFDM-IM is largely affected by the design of constellations. To obtain IM-preferable constellations, we propose two heuristic GCS approaches based on particle swarm optimization (PSO) and hybrid genetic algorithm-PSO (GA-PSO) algorithms. Without the loss of generality, we consider the design of 8-ary constellations for both OFDM-SM and OFDM-DM using the proposed heuristic GCS approaches. Since the position of each constellation point can be represented by its *X* and *Y* coordinates, heuristic GCS aims to minimize the BER by finding the optimal *X* and *Y* coordinates of each constellation point in the constellation. Hence, the PSO and GA-PSO algorithms optimize the constellation diagram by encapsulating the BER in the fitness value, while treating the sixteen *X* and *Y* coordinates corresponding to the eight constellation points as one particle.

2.2.1. PSO-based GCS

In the PSO algorithm, each particle engages in random exploration of the solution space and shares its discoveries with others, and the interactions between particles are designed to approach the global optimum closely [28]. The flow chart of the PSO-based GCS approach is depicted in Fig. 2, where random constellation points are first generated as the input and then the initial population is created. Subsequently, the particle position and velocity are updated iteratively until reaching the maximum number of iterations. Letting T denote the maximum number of iterations, for the ith iteration with $i = 1, \ldots, T$, the fitness value of each particle is first calculated and then the individual extreme value pbest and the group extreme value gbest of each particle are further calculated. In a population of J particles, the position P and velocity V of the jth $(j = 1, \ldots, J)$ particle at iteration i are expressed by

$$P^{j}(i) = \left[X^{j}(i), Y^{j}(i) \right], \tag{1}$$

$$V^{j}(i) = \left[v_{x}^{j}(i), v_{y}^{j}(i)\right]. \tag{2}$$

After determining the individual extreme value $pbest^{j}$ and the group extreme value $gbest^{j}$ of the jth particle at iteration i, the particle position, i.e., $X^{j}(i)$ and $Y^{j}(i)$, and the particle velocity $V^{j}(i)$ of each particle at iteration i + 1 are updated as follows:

$$X^{j}(i+1) = \left[X^{j}(i), v_{x}^{j}(i+1)\right],$$
 (3)

$$y^{j}(i+1) = \left[y^{j}(i), v_{y}^{j}(i+1) \right],$$
 (4)

$$V^{j}(i+1) = wV^{j}(i) + c_{1}r_{1} \left[pbest^{j} - P^{j}(i) \right] + c_{2}r_{2} \left[gbest^{j} - P^{j}(i) \right], \tag{5}$$

where w is the inertia weight chosen between 0 and 1; c_1 and c_2 are the cognitive and social coefficients, respectively; r_1 and r_2 are both random numbers between 0 and 1. Moreover, the inertia weight w is calculated by

$$w = w_{\text{max}} - \frac{(w_{\text{max}} - w_{\text{min}})i}{T},\tag{6}$$

where w_{max} and w_{min} are the maximum and minimum inertia weights, respectively.

Finally, after reaching the maximum number of iterations, the obtained optimal particle position, i.e., $X^{\text{opt}}(T)$ and $Y^{\text{opt}}(T)$, will be used to output the optimized constellation points.

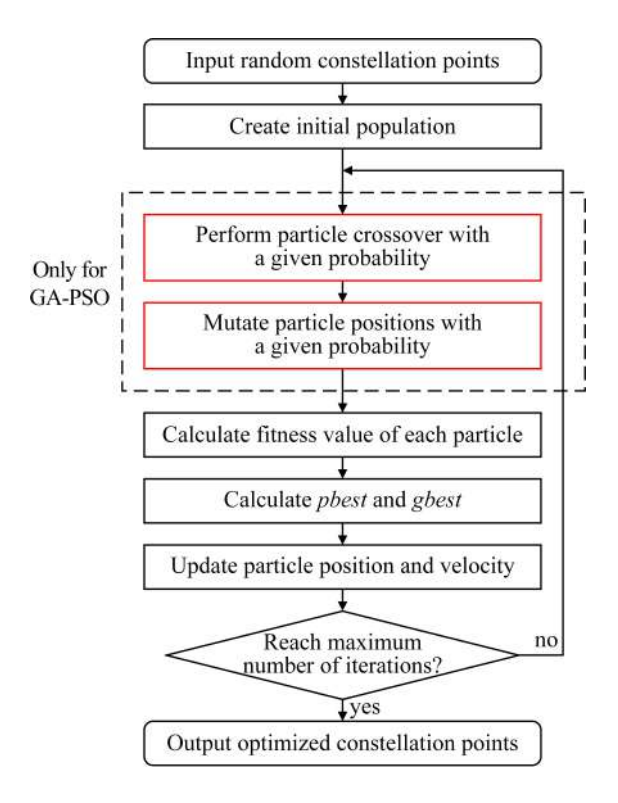


Fig. 2. Flow chart of the PSO-based/GA-PSO-based GCS approach

2.2.2. GA-PSO-based GCS

Considering that the PSO-based GCS approach is prone to premature convergence which might fall into a local optimality [29], the obtained constellation design using PSO-based GCS might have relatively poor performance. To address the disadvantage of the PSO algorithm, a hybrid algorithm combining PSO and GA can be utilized [30]. As a result, we further propose a hybrid GA-PSO-based GCS approach to enhance the performance of constellation design for both OFDM-SM and OFDM-DM.

The flow chart of the GA-PSO-based GCS approach is also depicted in Fig. 2, where the difference is that two additional blocks as plotted in red lines are added to implement the GA algorithm. Specifically, at the beginning of each iteration, particle crossover is first performed with a given probability and then particle positions are mutated with a given probability before calculating the fitness value, *pbest* and *gbest* and updating particle position and velocity. By introducing the GA algorithm, the proposed hybrid GA-PSO-based GCS approach can take full advantage of the global optimum-seeking nature of the GA algorithm and hence generate a constellation design with improved performance.

2.3. Generalized interleaving

Practical UVLC systems are generally bandlimited with a low-pass frequency response, which might degrade the BER performance of subblocks in the high-frequency region when applying OFDM-SM/DM. To address the adverse low-pass effect, we further propose a generalized interleaving technique for bandlimited UVLC systems using OFDM-SM/DM. Differing from traditional interleaving in which the neighboring subcarriers within each subblock are interleaved

sequentially with a step size the same as the subblock length, the proposed generalized interleaving technique introduces a variable step size to perform subblock interleaving.

Figure 3 illustrates the OFDM-IM spectrum using generalized interleaving by taking N = 4and G = 4 as an example. For a step size of 1, as shown in Fig. 3(a), different subblocks are sequentially placed within the signal bandwidth and hence it is equivalent to the case without interleaving. For a step size of 2, as given in Fig. 3(b), the four subcarriers in the first subblock are placed at the subcarrier slots 1, 3, 5 and 7, while the four subcarriers in the second subblock occupy the subcarrier slots 9, 11, 13 and 15. Since there are only a total of N_{data} =16 subcarriers, the four subcarriers in the third subblock are placed at the subcarrier slots 2, 4, 6 and 8, while the four subcarriers in the fourth subblock occupy the subcarrier slots 10, 12, 14 and 16. Following the same manner, we can perform generalized interleaving for a step size of 3, as can be seen Fig. 3(c). When the step size is increased to the subblock length, i.e., step = 4, as depicted in Fig. 3(d), the generalized interleaving becomes exactly the traditional interleaving. As a result, no interleaving and traditional interleaving can be seen as two extreme cases of the proposed generalized interleaving technique. Moreover, the step size to perform generalized interleaving can be treated as a variable and an optimal step size can be identified to yield the best BER performance of the overall system. Although the principle of the proposed generalized interleaving technique is illustrated by taking N = 4 and G = 4 as an example, it is feasible to apply generalized interleaving in a general OFDM-IM system.

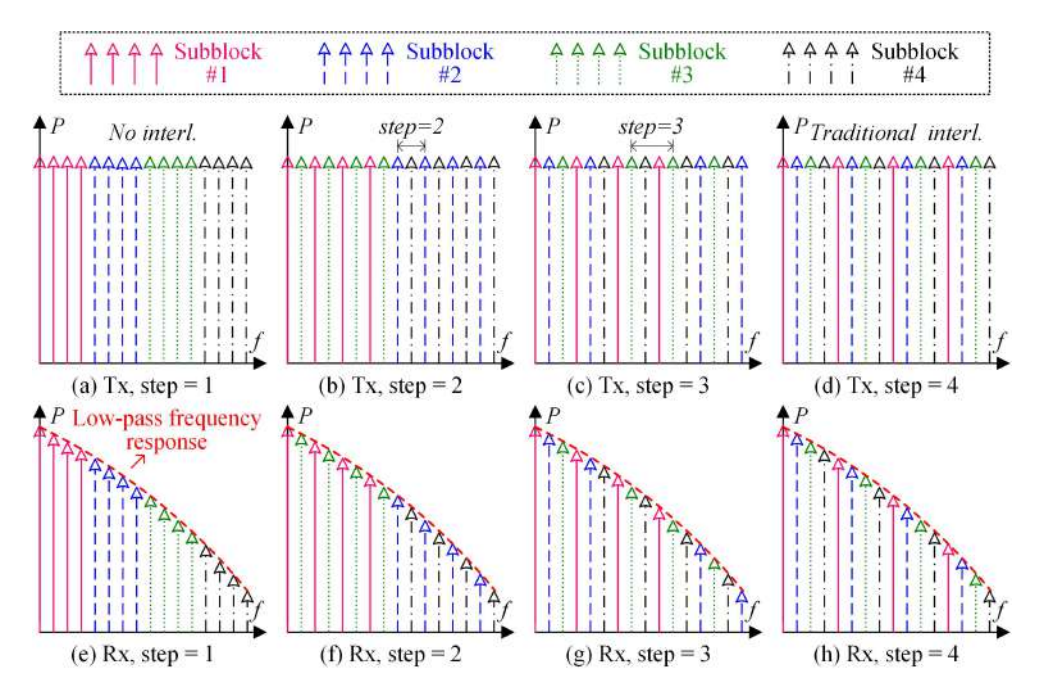


Fig. 3. Illustration of OFDM-IM spectrum using generalized interleaving by taking N = 4 and G = 4 as an example: (a) Tx, step = 1, (b) Tx, step = 2, (c) Tx, step = 3, (d) Tx, step = 4, (e) Rx, step = 1, (f) Rx, step = 2, (g) Rx, step = 3, and (h) Rx, step = 4.

3. Results and discussions

3.1. Simulation results

In the simulations, we consider a bandlimited UVLC system over an additive white Gaussian noise (AWGN) channel. The size of IFFT/FFT, the number of data subcarriers and the length of

each subblock in OFDM-SM/DM are set to 128, 60 and 4. respectively. To ensure the general applicability of the constellations obtained via the proposed heuristic GCS approaches, the PSO-based/GA-PSO-based GCS is performed over the AWGN channel without considering the low-pass frequency response of the bandlimited UVLC system. Considering the relatively high computation complexity to perform PSO-based/GA-PSO-based GCS, it might not be feasible to adaptively perform PSO-based/GA-PSO-based GCS according to the change of the low-pass effect in practical UVLC systems. Specifically, the PSO algorithm is executed with a maximum inertia weight w_{max} of 0.8, a minimum inertia weight w_{min} of 0.4, a maximum velocity V_{max} of 4, a dimension of 16 and a learning factor of 1.5, while the GA algorithm is performed with a crossover probability of 0.1 and a variance probability of 0.001. In addition, the SNRs selected to perform PSO-based GCS for OFDM-SM, GA-PSO-based GCS for OFDM-SM, PSO-based GCS for OFDM-DM and GA-PSO-based GCS for OFDM-DM are 9.8, 9.5, 11.3 and 11 dB, respectively. These SNRs are selected to ensure that the resultant BERs are near the 7% forward error correction (FEC) coding threshold of BER = 3.8×10^{-3} . Moreover, the proposed generalized interleaving technique is optimized by finding the optimal step size and the optimization is performed over the AWGN channel with the low-pass frequency response of the bandlimited UVLC system. It should be noted that the optimal step size to perform generalized interleaving in practical bandlimited UVLC systems can be easily obtained via the following two steps: 1) estimating the low-pass effect experienced by the OFDM-IM signal via channel estimation; 2) performing simulation using the estimated low-pass effect to obtain the optimal step size that can yield the minimum BER. Since the simulation process to find the optimal step size has relatively low computational complexity, it can be adaptively performed according to the change of the low-pass effect in practical bandlimited UVLC systems.

Figures 4(a) and (b) show the optimization processes of two heuristic GCS approaches for OFDM-SM and OFDM-DM, respectively. As we can see, compared with the PSO-based GCS approach, the GA-PSO-based GCS approach requires a smaller number of iterations to reach the 7% FEC coding limit of BER = 3.8×10^{-3} for both OFDM-SM and OFDM-DM cases, indicating that the use of hybrid GA-PSO algorithm can obtain a faster convergence speed than the use of PSO only. Furthermore, it can also been found that the GA-PSO-based GCS approach can achieve a lower BER than the PSO-based GCS approach after 20 iterations for both OFDM-SM and OFDM-DM cases, which shows the improved performance of the designed constellation due to the global optimum-seeking nature of the GA algorithm.

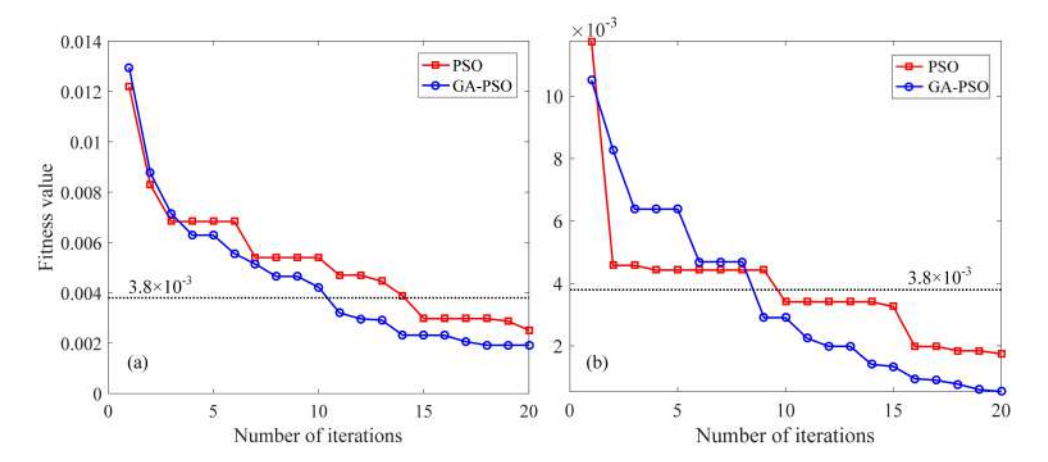


Fig. 4. Simulation fitness value vs. number of iterations of PSO-based and GA-PSO-based GCS approaches for (a) OFDM-SM and (b) OFDM-DM.

Figure 5 depicts the adopted constellations for OFDM-SM/DM in bandlimited UVLC systems. For OFDM-SM, 8QAM and 8-ary phase-shift keying (8PSK) are considered as benchmark constellations, while the obtained constellations using PSO-based GCS and GA-PSO-based GCS are given by Figs. 5(c) and (d), respectively. For OFDM-DM, dual-mode 8QAM and 8PSK are adopted for comparison, while the obtained dual-mode constellations using PSO-based GCS and GA-PSO-based GCS are given by Figs. 5(g) and (h), respectively. As we can observe, the constellations obtained via both PSO-based GCS and GA-PSO-based GCS generally exhibit irregular shapes, which might achieve better performance than the benchmark constellations.

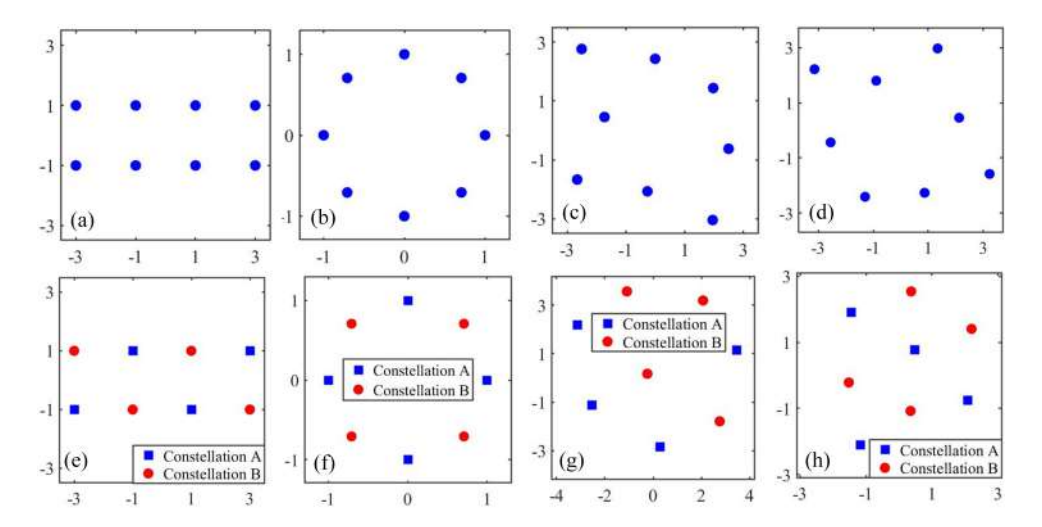


Fig. 5. Constellations for OFDM-SM: (a) 8QAM, (b) 8PSK, (c) using PSO-based GCS, and (d) using GA-PSO-based GCS, and constellations for OFDM-DM: (e) 8QAM, (f) 8PSK, (g) using PSO-based GCS, and (h) using GA-PSO-based GCS.

Figures 6(a) and (b) compare the PAPR performance using different constellation designs for OFDM-SM and OFDM-DM, respectively. As we can see, for both OFDM-SM and OFDM-DM, comparable PAPR performance can be obtained by using different constellation designs.

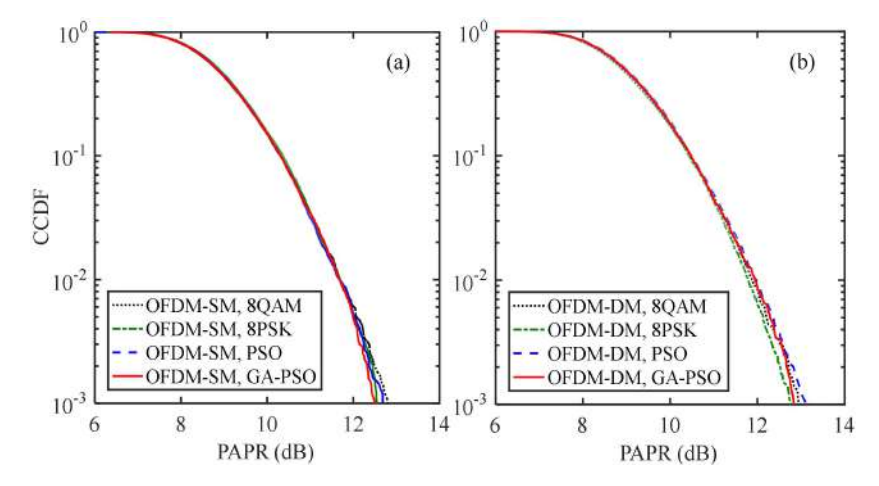


Fig. 6. PAPR performance using different constellation designs for (a) OFDM-SM and (b) OFDM-DM.

Figures 7(a) and (b) show the simulation BER versus SNR using different constellation designs for OFDM-SM and OFDM-DM, respectively. For the case of OFDM-SM, as shown in Fig. 7(a), 8QAM performs the worst while the constellation obtained via GA-PSO-based GCS achieves the best performance among all the considered constellations. Moreover, the constellation obtained via PSO-based GCS can only slightly outperform 8PSK and further performance improvement can be observed when using GA-PSO-based GCS. More specifically, a 0.76-dB SNR gain is achieved by the constellation obtained via GA-PSO-based GCS in comparison to 8PSK. For the case of OFDM-DM, as can be seen from Fig. 7(b), dual-mode 8PSK has the worst performance while the dual-mode constellation obtained via GA-PSO-based GCS still performs the best. Compared with dual-mode 8QAM, the dual-mode constellation obtained via GA-PSO-based GCS achieves an SNR gain of 0.92 dB. It can be generally found from Fig. 7 that the proposed heuristic GCS approaches can efficiently generate performance-enhanced constellations for both OFDM-SM and OFDM-DM, and GA-PSO-based GCS outperforms PSO-based GCS due to introduction of the GA algorithm.

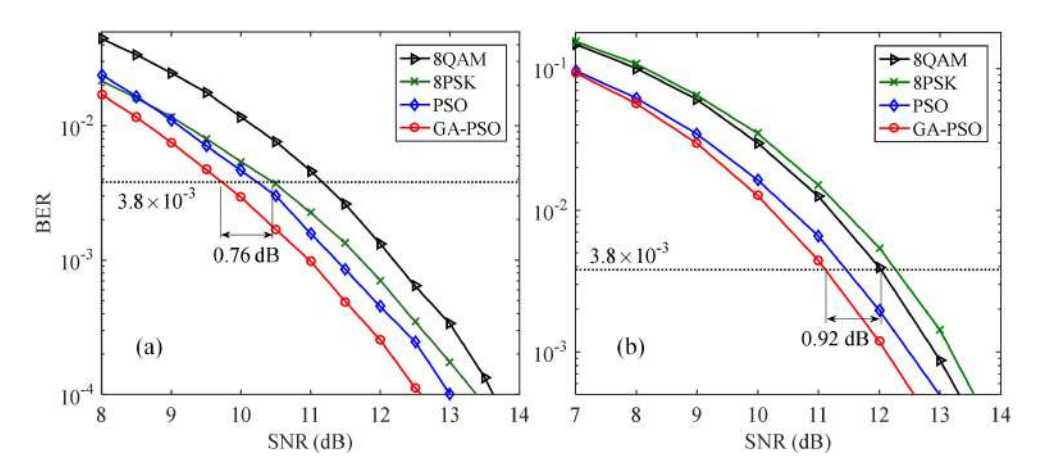


Fig. 7. Simulation BER vs. SNR using different constellation designs for (a) OFDM-SM and (b) OFDM-DM.

In order to optimize the step size when performing generalized interleaving, a practical low-pass frequency response measured from the experimental UVLC system is considered, which is plotted in Fig. 8. Figures 9(a) and (b) show the simulation BER versus step size in generalized interleaving with different SNR values for OFDM-SM and OFDM-DM, respectively. As we can see, the BER first decreases and then increases with the increase of the step size from 1 to 15 for both OFDM-SM and OFDM-DM, and the optimal step sizes for the two cases are both 4. Moreover, the optimal step size remains the same when changing the SNR values for both OFDM-SM and OFDM-DM, which might be mainly determined by the adopted low-pass frequency response in simulations.

3.2. Experimental results

We further conduct hardware experiments to evaluate the performance of the proposed enhanced OFDM-IM scheme and compare it with other benchmark schemes by configuring an experimental UVLC system. The experimental setup of the UVLC system is depicted in Fig. 10, where the transmitted signal generated offline by MATLAB is first loaded to an arbitrary waveform generator (AWG, Tektronix AFG31102) with a sampling rate of 10 MSa/s. The AWG output is fed to the AC port of an optical transmitter (Tx) module, which is powered by a 12-V DC bias voltage. The emitted light passes through a 1-meter water tank filled with tap water and

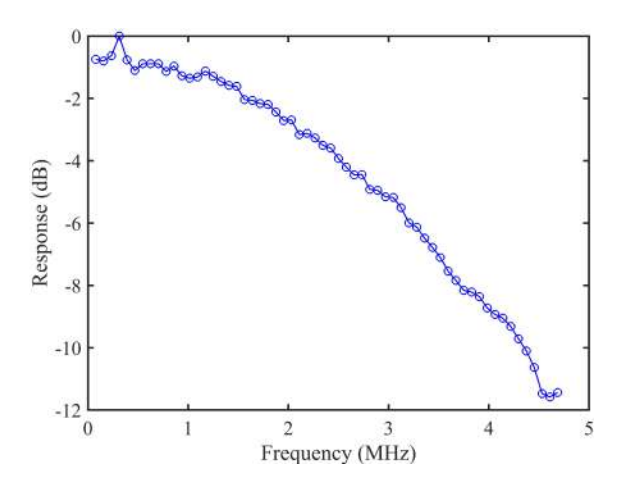


Fig. 8. Low-pass frequency response measured from the experimental UOWC system.

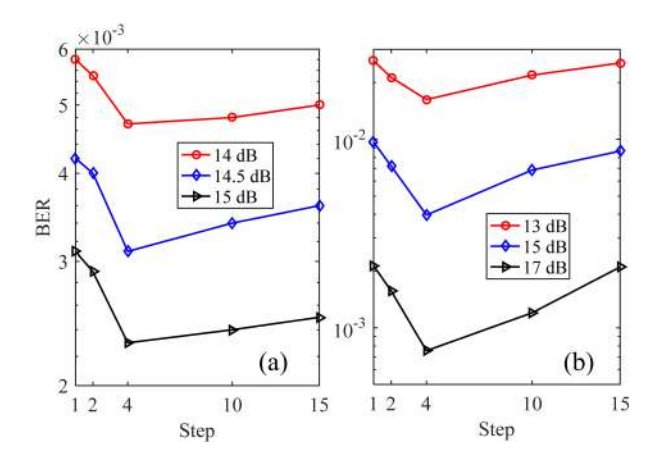


Fig. 9. Simulation BER vs. step size in generalized interleaving for (a) OFDM-SM and (b) OFDM-DM.

an optical receiver (Rx) module is used to detect the light signal, which is also powered by a 12-V DC bias voltage. The detected signal is recorded by a digital storage oscilloscope (DSO, Tektronix MDO32) with a sampling rate of 50 MSa/s and the obtained data are further processed offline using MATLAB. In OFDM-IM modulation, the IFFT/FFT size is 128 and the number of data subcarriers is 60. As a result, the effective signal bandwidth is about 4.7 MHz. The low-pass frequency response of the experimental UVLC system is illustrated in Fig. 8. In the experiments, a optimal step size of 4 is adopted to perform generalized interleaving in the proposed enhanced OFDM-IM scheme.

Figures 11(a) and (b) show the measured BER versus received SNR with different constellations without and with interleaving for OFDM-SM and OFDM-DM, respectively. For OFDM-SM, as shown in Fig. 11(a), 8QAM without interleaving cannot reach the 7% FEC coding limit of BER = 3.8×10^{-3} within the received SNR range from 13.4 to 15.8 dB, and 8PSK without interleaving requires an SNR of 15.4 dB to reach BER = 3.8×10^{-3} . Moreover, the constellation obtained via PSO-based GCS without interleaving has comparable performance as 8QAM without interleaving, while the constellation obtained via GA-PSO-based GCS without interleaving slightly outperforms that obtained via PSO-based GCS without interleaving. It can be seen

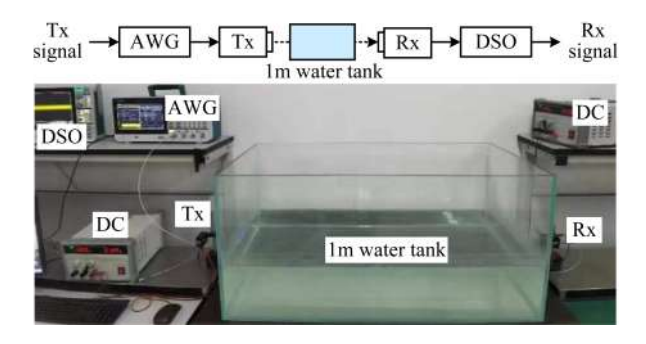


Fig. 10. Experimental setup of the UVLC system.

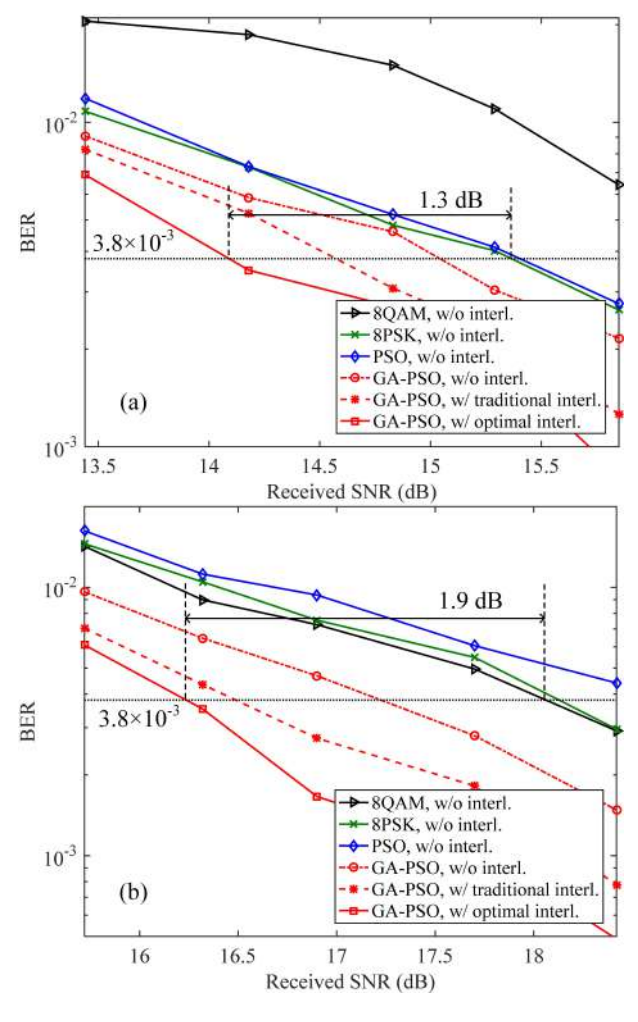


Fig. 11. Measured BER vs. SNR with different constellations without and with interleaving for (a) OFDM-SM and (b) OFDM-DM.

that further performance improvement can be obtained by applying subblock interleaving to mitigate the adverse effect of the low-pass frequency response of the system. More specifically, the required SNRs for the constellation obtained via GA-PSO-based GCS using traditional

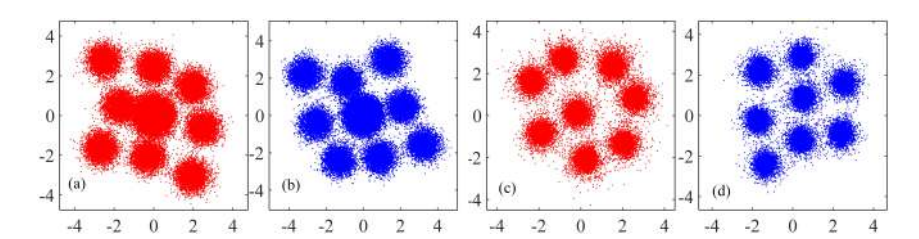


Fig. 12. Received constellation diagrams for (a) OFDM-SM, PSO, 15.3 dB, (b) OFDM-SM, GA-PSO, 15.3 dB, (c) OFDM-DM, PSO, 18.4 dB, and (d) OFDM-DM, GA-PSO, 18.4 dB.

interleaving and generalized interleaving with an optimal step size of 4 are 14.6 and 14.1 dB, respectively. Hence, optimal interleaving outperforms traditional interleaving with an SNR gain of 0.5 dB. Compared with 8PSK without interleaving, the constellation obtained via GA-PSO-based GCS using optimal interleaving can achieve an SNR gain of 1.3 dB. For OFDM-DM, as can be seen from Fig. 11(b), the constellation obtained via PSO-based GCS without interleaving cannot reach BER = 3.8×10^{-3} within the received SNR range from 15.7 to 18.4 dB, while the constellation obtained via GA-PSO-based GCS without interleaving requires an SNR of 17.2 dB to reach BER = 3.8×10^{-3} . Similarly, the use of subblock interleaving can efficiently mitigate the low-pass effect and hence improve the BER performance. Particularly, the constellation obtained via GA-PSO-based GCS using traditional interleaving and optimal interleaving requires SNRs of 16.5 and 16.2 dB to meet the BER threshold, respectively. As a result, a remarkable 1.9-dB SNR gain can be achieved by the constellation obtained via GA-PSO-based GCS with optimal interleaving in comparison to 8QAM without interleaving. It can be concluded from Fig. 11 that both GA-PSO-based GCS and generalized interleaving are effective techniques to enhance the performance of OFDM-IM in bandlimited UVLC systems. Figure 12 depicts the received constellation diagrams for OFDM-SM and OFDM-DM using PSO-based/GA-PSO-based GCS.

4. Conclusion

In this paper, we have proposed and evaluated enhanced OFDM-IM schemes for bandlimited UVLC systems, where heuristic GCS and generalized interleaving are considered to obtain performance-enhanced constellations for OFDM-IM and address the low-pass effect of system, respectively. For the heuristic GCS approaches, two heuristic algorithms including PSO and GA-PSO are utilized to perform the constellation design. For generalized interleaving, the step size is treated as a optimization parameter to yield the best interleaving performance. The feasibility and superiority of the proposed enhanced OFDM-IM schemes have been successfully verified via both simulation and experiments. Therefore, the proposed enhanced OFDM-IM schemes can be promising for the application in practical bandlimited UVLC systems.

Funding. National Natural Science Foundation of China (61901065, 62271091); Natural Science Foundation of Chongqing (cstc2021jcyj-msxmX0480).

Disclosures. The authors declare no conflicts of interest.

Data availability. The data underlying the results presented in this paper are not publicly available at this time but may be obtained from the authors upon reasonable request.

References

- 1. N. Chi, Y. Zhou, Y. Wei, *et al.*, "Visible light communication in 6G: Advances, challenges, and prospects," IEEE Veh. Technol. Mag. **15**(4), 93–102 (2020).
- M. V. Jamali, P. Nabavi, and J. A. Salehi, "MIMO underwater visible light communications: Comprehensive channel study, performance analysis, and multiple-symbol detection," IEEE Trans. Veh. Technol. 67(9), 8223–8237 (2018).
- 3. Z. Zeng, S. Fu, H. Zhang, *et al.*, "A survey of underwater optical wireless communications," IEEE Commun. Surv. Tutorials **19**(1), 204–238 (2017).

- 4. M. Elamassie, F. Miramirkhani, and M. Uysal, "Performance characterization of underwater visible light communication," IEEE Trans. Commun. 67(1), 543–552 (2019).
- M. F. Ali, D. N. K. Jayakody, and Y. Li, "Recent trends in underwater visible light communication (UVLC) systems," IEEE Access 10, 22169–22225 (2022).
- S. Hessien, S. C. Tokgöz, N. Anous, et al., "Experimental evaluation of OFDM-based underwater visible light communication system," IEEE Photonics J. 10(5), 1–13 (2018).
- Y. Li, H. Qiu, X. Chen, et al., "A novel PAPR reduction algorithm for DCO-OFDM/OQAM system in underwater VLC," Opt. Commun. 463, 125449 (2020).
- 8. E. Basar, U. Aygolu, E. Panayirci, *et al.*, "Orthogonal frequency division multiplexing with index modulation," IEEE Trans. Signal Process. **61**(22), 5536–5549 (2013).
- 9. M. Wen, X. Cheng, M. Ma, et al., "On the achievable rate of OFDM with index modulation," IEEE Trans. Signal Process. 64(8), 1919–1932 (2016).
- 10. T. Mao, Z. Wang, Q. Wang, et al., "Dual-mode index modulation aided OFDM," IEEE Access 5, 50-60 (2017).
- 11. E. Başar and E. Panayırcı, "Optical OFDM with index modulation for visible light communications," in *IEEE Int. Workshops Opt. Wireless Commun.*, (2015), pp. 11–15.
- T. Mao, R. Jiang, and R. Bai, "Optical dual-mode index modulation aided OFDM for visible light communications," Opt. Commun. 391, 37–41 (2017).
- C. Chen, X. Deng, Y. Yang, et al., "Experimental demonstration of optical OFDM with subcarrier index modulation for IM/DD VLC," in Asia Communications and Photonics Conference, (2019), p. M4A.40.
- F. Ahmed, Y. Nie, C. Chen, et al., "DFT-spread OFDM with quadrature index modulation for practical VLC systems," Opt. Express 29(21), 33027–33036 (2021).
- Z. A. Qasem, A. Ali, B. Deng, et al., "Index modulation-based efficient technique for underwater wireless optical communications," Opt. Laser Technol. 167, 109683 (2023).
- Z. A. Qasem, A. Ali, B. Deng, et al., "Unipolar X-transform OFDM with index modulation for underwater optical wireless communications," IEEE Photonics Technol. Lett. 35(11), 581–584 (2023).
- 17. Y. Nie, C. Chen, S. Savović, et al., "0.5-bit/s/Hz fine-grained adaptive OFDM modulation for bandlimited underwater VLC," Opt. Express 32(3), 4537–4552 (2024).
- C. Chen, Y. Nie, F. Ahmed, et al., "Constellation design of DFT-S-OFDM with dual-mode index modulation in VLC," Opt. Express 30(16), 28371–28384 (2022).
- A. Mirani, E. Agrell, and M. Karlsson, "Low-complexity geometric shaping," J. Lightwave Technol. 39(2), 363–371 (2021).
- E. Sillekens, G. Liga, D. Lavery, et al., "High-cardinality geometrical constellation shaping for the nonlinear fibre channel," J. Lightwave Technol. 40(19), 6374

 –6387 (2022).
- P. Zou, Y. Liu, F. Wang, et al., "Enhanced performance of odd order square geometrical shaping QAM constellation in underwater and free space VLC system," Opt. Commun. 438, 132–140 (2019).
- 22. P. Zou, Y. Zhao, F. Hu, *et al.*, "Square geometrical shaping 128QAM based time domain hybrid modulation in visible light communication system," China Commun. **17**(1), 163–173 (2020).
- B. Chen, Y. Lei, G. Liga, et al., "Geometrically-shaped multi-dimensional modulation formats in coherent optical transmission systems," J. Lightwave Technol. 41(3), 897–910 (2023).
- 24. B. Chen, W. Ling, Y. Lei, *et al.*, "Orthant-symmetric four-dimensional geometric shaping for fiber-optic channels via a nonlinear interference model," Opt. Express **31**(10), 16985–17002 (2023).
- 25. Z. Liang, B. Chen, Y. Lei, et al., "Analytical model of nonlinear fiber propagation for general dual-polarization four-dimensional modulation formats," J. Lightwave Technol. 42(2), 606–620 (2024).
- Y. Nie, J. Chen, W. Wen, et al., "Orthogonal subblock division multiple access for OFDM-IM-based multi-user VLC systems," Photonics 9(6), 373 (2022).
- J. Chen, B. Deng, C. Chen, et al., "Efficient capacity enhancement using OFDM with interleaved subcarrier number modulation in bandlimited UOWC systems," Opt. Express 31(19), 30723–30734 (2023).
- 28. R. Poli, J. Kennedy, and T. Blackwell, "Particle swarm optimization: An overview," Swarm Intell. 1(1), 33-57 (2007).
- A. Banks, J. Vincent, and C. Anyakoha, "A review of particle swarm optimization. Part I: background and development," Nat. Comput. 6(4), 467–484 (2007).
- 30. R. C. Eberhart and Y. Shi, "Comparison between genetic algorithms and particle swarm optimization," in *International conference on evolutionary programming*, (1998), pp. 611–616.